

Accepted Manuscript

Changes in Regional Ventilation during Treatment and Dosimetric Advantages of CT Ventilation Image-Guided Radiotherapy for Locally Advanced Lung Cancer

Tokihiro Yamamoto, Ph.D., Sven Kabus, Ph.D., Matthieu Bal, Ph.D., Karl Bzdusek, Ph.D., Paul J. Keall, Ph.D., Cari Wright, B.S., Stanley H. Benedict, Ph.D., Megan E. Daly, M.D.

PII: S0360-3016(18)30741-7

DOI: [10.1016/j.ijrobp.2018.04.063](https://doi.org/10.1016/j.ijrobp.2018.04.063)

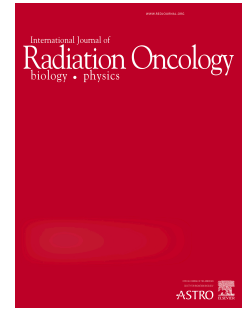
Reference: ROB 24972

To appear in: *International Journal of Radiation Oncology • Biology • Physics*

Received Date: 9 December 2017

Please cite this article as: Yamamoto T, Kabus S, Bal M, Bzdusek K, Keall PJ, Wright C, Benedict SH, Daly ME, Changes in Regional Ventilation during Treatment and Dosimetric Advantages of CT Ventilation Image-Guided Radiotherapy for Locally Advanced Lung Cancer, *International Journal of Radiation Oncology • Biology • Physics* (2018), doi: 10.1016/j.ijrobp.2018.04.063.

This is a PDF file of an unedited manuscript that has been accepted for publication. As a service to our customers we are providing this early version of the manuscript. The manuscript will undergo copyediting, typesetting, and review of the resulting proof before it is published in its final form. Please note that during the production process errors may be discovered which could affect the content, and all legal disclaimers that apply to the journal pertain.



Changes in Regional Ventilation during Treatment and Dosimetric Advantages of CT Ventilation Image-Guided Radiotherapy for Locally Advanced Lung Cancer

5 Tokihiro Yamamoto, Ph.D.,¹ Sven Kabus, Ph.D.,² Matthieu Bal, Ph.D.,³ Karl Bzdusek,⁴ Ph.D., Paul J. Keall, Ph.D.,⁵ Cari Wright, B.S.,¹ Stanley H. Benedict, Ph.D.,¹ and Megan E. Daly, M.D.¹

¹Department of Radiation Oncology, University of California Davis, Sacramento,
10 California

²Department of Digital Imaging, Philips Research, Hamburg, Germany

³Philips Healthcare, Best, The Netherlands

⁴Philips Healthcare, Fitchburg, WI

⁵Radiation Physics Laboratory, Sydney Medical School, University of Sydney, New
15 South Wales, Australia

Reprint request to: Tokihiro Yamamoto, Ph.D., Department of Radiation Oncology,
University of California Davis, 4501 X St., Sacramento, California 95817. Tel: (916)
734-0604; E-mail: toyamamoto@ucdavis.edu

20

Short title: Ventilation image-guided adaptive radiotherapy

Funding: This study was supported in part by the American Cancer Society and the Dean of the UC Davis School of Medicine (ACS IRG-95-125-13) (T.Y. and M.E.D.) and
25 National Institutes of Health/National Cancer Institute grant K12CA138464 (M.E.D.).

Acknowledgment: Philips Radiation Oncology Systems loaned us a research version of the Pinnacle³ treatment planning system.

30 **Conflict of interest:** Drs. Kabus, Bal and Bzdusek are employees of Philips. Dr. Keall is an inventor of the issued patent, Method and system for using computed tomography to test pulmonary function (US 7668357).

Abstract

Purpose/Objective: Lung functional image-guided radiotherapy (RT) that avoids irradiating highly-functional regions has potential to reduce pulmonary toxicity following RT. Tumor regression during RT is common, leading to recovery of lung function. We hypothesized that
5 computed tomography (CT) ventilation image-guided treatment planning reduces the functional lung dose compared to standard anatomical image-guided planning in two different scenarios with or without plan adaptation.

Methods and Materials: CT scans were acquired before RT and during RT at two time points (16-20 Gy and 30-34 Gy) for 14 patients with locally advanced lung cancer. Ventilation images
10 were calculated by deformable image registration (DIR) of four-dimensional (4D) CT image datasets and image analysis. We created four treatment plans at each time point for each patient: functional adapted, anatomical adapted, functional unadapted, and anatomical unadapted plans. Adaptation was performed at two time points. DIR was used for accumulating dose and calculating a composite of dose-weighted ventilation used to quantify
15 the lung accumulated dose-function metrics. The functional plans were compared with the anatomical plans for each scenario separately to investigate the hypothesis at a significance level of 0.05.

Results: Tumor volume was significantly reduced by 20% after 16-20 Gy ($p=0.02$) and by 32% after 30-34 Gy ($p<0.01$) on average. In both scenarios, the lung accumulated dose-function
20 metrics were significantly lower in the functional plans than in the anatomical plans without compromising target volume coverage and adherence to constraints to critical structures. For example, functional planning significantly reduced the functional mean lung dose by 5.0% ($p<0.01$) compared to anatomical planning in the adapted scenario, and by 3.6% ($p=0.03$) in the unadapted scenario.

Conclusions: This study demonstrated significant reductions in the accumulated dose to the
25 functional lung with CT ventilation image-guided planning compared to anatomical image-

guided planning for patients showing tumor regression and changes in regional ventilation during RT.

ACCEPTED MANUSCRIPT

30 Introduction

Radiotherapy (RT) for lung cancer is limited by substantial pulmonary toxicity that diminishes quality of life [1-3], particularly for locally advanced disease. Common toxicities include radiation pneumonitis (potentially fatal) that occurs in up to 30-40% of patients irradiated for locally advanced lung cancer [3,4], pulmonary fibrosis that occurs in about 8% [4,5], and lung
35 function loss, e.g., 4-27% reduction in diffusing capacity of the lung for carbon monoxide (DL_{CO}) [1,6]. Lung functional image-guided RT, which preferentially avoids irradiating highly-functional lung regions, has potential to reduce pulmonary toxicity, and thereby improve quality of life. Dosimetric significance of lung functional image-guided RT has been demonstrated by several investigators [7-11]. Recently, Faught *et al.* translated the reduction in the functional lung dose
40 to an estimated reduction in the risk of severe pneumonitis by 5-8% on average for the population and as high as 52% for individual patients (clinically-used anatomical image-guided planning without adaptation versus functional image-guided planning without adaptation) [12]. Other key evidence that supports functional image-guided RT includes improved toxicity prediction based on regional ventilation and perfusion [13,14], and dose-dependent reductions
45 in regional ventilation and perfusion after RT [15,16].

Many lung cancer patients experience tumor shrinkage during a course of RT at a rate of 0.6-2.4% per day (tumor volume) [17]. Several investigators have reported significant increases in regional ventilation and perfusion during a course of RT for lung cancer, and speculated that
50 those changes might be attributed to re-opening of airways and vessels as a result of tumor shrinkage [18-20]. Yuan *et al.* reported significant reductions in ventilation and perfusion defects measured with single-photon emission computed tomography (SPECT) imaging after 45 Gy compared to pre-RT images [19]. These findings suggest that functional image-guided unadapted plans might end up with little reduction in the accumulated dose to the functional
55 lung, as dose is redistributed to regions that are poorly functional before RT but may become

functional during RT. There have been no studies to quantify the dosimetric impact of changes in regional lung function during RT. Also, adaptive RT strategies to account for such changes during RT [21-23] have not been investigated for functional image-guided RT.

60 Several modalities exist for pulmonary ventilation imaging, including an emerging method based on four-dimensional (4D) computed tomography (CT) and image processing (henceforth referred to as CT ventilation imaging). CT ventilation imaging has higher resolution, shorter exam time, lower cost, and greater availability compared to other modalities. CT ventilation can often be considered 'free' information in RT, as 4D CT is in routine use for respiratory motion
65 assessment in RT planning at many centers (approximately 70% of RT centers in the US [24]) and ventilation computation only involves image processing and analysis. Therefore, CT ventilation imaging has great potential for widespread clinical implementation. The accuracy and precision of CT ventilation imaging have been investigated extensively through animal studies [25-27] and human studies [27-37]. Reasonable correlations with pulmonary function
70 tests (PFTs) [33,35] and ventilation images acquired with other methods [25,26,28,30,32-34,37] indicate the physiological significance of CT ventilation imaging. For example, Brennan *et al.* found moderate to strong correlations (range: 0.63-0.72) between the CT ventilation metrics (e.g., coefficient of variation, the relative volume of lung with $\leq 20\%$ ventilation) and PFT parameters (e.g., forced expiratory volume in 1 second) in a 98-patient study [35].

75 The purpose of this study was to quantify the dosimetric advantages of CT ventilation functional image-guided RT planning for locally advanced lung cancer in two different scenarios with or without plan adaptation. We hypothesized that CT ventilation image-guided treatment planning reduces the functional lung dose compared to standard anatomical image-guided planning in
80 both scenarios.

Methods and Materials

Patients

In an ongoing prospective clinical trial approved by the institutional review board (*detail omitted*
85 *for blind review*) evaluating the feasibility of CT ventilation functional image-guided RT, 14
patients with stage III non-small cell lung cancer (NSCLC) underwent protocol-defined, mid-RT
4D CT scans as well as planning 3D CT scans at two time points (after 16-20 Gy and 30-34 Gy)
in addition to pre-RT scans. All patients were treated with functional image-guided plans
without adaptation per protocol, and provided written informed consent prior to enrollment.
90 Table 1 summarizes patient characteristics.

Imaging

All CT scans were acquired using a Brilliance Big Bore multislice CT scanner (Philips
Healthcare, Andover, MA). For 4D CT, the respiratory signal was acquired using a pneumatic
95 belt and the following scanning parameters were used consistently: 120 kVp, 120 mA, and 2
mm slice. Although breathing guidance (*e.g.*, audiovisual biofeedback) was not used in this
study, we provided verbal instruction to patients to maintain regular breathing. The B (standard)
algorithm was used for image reconstruction. The phase-based method was used for 4D CT
sorting. Patients were positioned using the same patient-specific immobilization devices
100 throughout all CT scans to reduce variability in positioning.

CT ventilation imaging

CT ventilation imaging is based on (1) DIR of 4D CT image datasets and (2) quantitative image
analysis for regional volume change as a surrogate for ventilation. DIR was performed between
105 the selected inhale 4D CT image data set (moving) to the peak-exhale image data set (fixed) to
ensure consistency in the tidal volume between three different time points of 4D CT scans, *i.e.*,
equivalent tidal volume (ETV) normalization [38]. Du *et al.* found significantly improved

reproducibility in ETV-normalized CT ventilation compared to peak-inhale/exhale CT ventilation, when tidal volume variations were greater than 150 cm³ [38]. In this study, the inhale phase was selected such that tidal volume variations were smaller than 150 cm³. The tidal volume was determined by subtracting the volume of segmented lung in the peak-exhale image from that of a given inhale image. DIR was performed using a volumetric elastic algorithm that minimizes both a similarity function (sum of squared difference between) and a regularization term (elastic regularization) [39]. The accuracy of this algorithm has been previously evaluated thoroughly [39-41] and shown to have sub-voxel accuracy on average [40]. The same level of accuracy was assumed in this study, and only visual inspection of subtraction images (fixed minus deformed moving) was performed to check for major errors. No major errors were observed in this study, except for some local errors around 4D CT image artifacts (see the Discussion section). Regional ventilation was quantified using the Hounsfield unit (HU)-based metric [42,43] scaled by a local CT density [32,33]. Ventilation values were converted into percentile values for intensity-modulated RT (IMRT) planning as well as data analysis in this study. See Appendix e1 for further details on CT ventilation imaging.

Treatment planning and plan adaptation

We created four IMRT plans at each time point for each patient: (1) functional image-guided planning with plan adaptation, (2) anatomical image-guided planning with adaptation, (3) functional image-guided planning without adaptation, and (4) anatomical image-guided planning without adaptation. Contouring of the target volumes and critical structures was performed manually on the planning CT image at each time point. The gross tumor volume (GTV), which was defined as the primary tumor and any regionally involved lymph nodes identified by the planning CT image at each time point, was contoured by the same thoracic radiation oncologist (*detail omitted for blind review*) for all cases. The internal target volume (ITV) was defined as the envelope that encompassed the GTV plus a full range of motion of the primary tumor and

nodal target identified by 4D CT. The clinical target volume (CTV) was determined by adding a
135 margin of 5 mm to the ITV at each time point, assuming that the microscopic disease shrank
synchronously with the GTV [21,22]. The planning target volume (PTV) was determined by
adding an additional margin of 5 mm to the CTV. Major critical structures contoured include the
lungs, spinal cord, esophagus, and heart.

140 All IMRT plans were created by the same dosimetrist (*detail omitted for blind review*) with
coplanar or non-coplanar 6 MV photon beams on the planning CT image at each time point, *i.e.*,
pre-RT and mid-RT (16-20 Gy and 30-34 Gy). The dose of 60 Gy was prescribed to 95% of the
PTV. To ensure consistency in target volume coverage between the paired plans in each
scenario, all treatment plans (except for the mid-RT unadapted plans) were designed to meet
145 the following dose specifications at each time point: (1) the minimum dose to the PTV must be
 $\geq 90\%$ of the prescription dose, and (2) the maximum dose to the PTV must be $\leq 115\%$ of the
prescription dose. The isocenter was placed approximately in the target centroid position in the
pre-RT planning CT image. The same position relative to the triangulation setup marks was
used to place the isocenter in the 16-20 Gy and 30-34 Gy planning CT images. Functional
150 plans were designed to preferentially avoid irradiating highly-functional lung regions and meet
standard dose-volume constraints, while anatomical plans were designed to meet standard
constraints only. See Appendix e11 for the standard dose-volume constraints to major critical
structures. Functional image-guided planning was performed with lung dose-function objectives
that incorporated regional percentile ventilation values [36], *i.e.*, the image/voxel-based method
155 rather than the structure-based method. Beam angles were also optimized manually to avoid
passing through highly-functional lung regions. Plan adaptation was performed after both 16-20
Gy and 30-34 Gy. Unadapted plans were generated by simply copying the beams of the pre-RT
plan onto the isocenters of the 16-20 Gy and 30-34 Gy planning CT images. The Pinnacle³

treatment planning system, research version 9.7 (Philips Radiation Oncology Systems,
 160 Fitchburg, WI) was used in this study.

Dose accumulation

Dose accumulation was performed with the Demons DIR algorithm of the Pinnacle³ treatment
 planning system (research version 9.7), which was used to warp the mid-RT dose distributions
 165 as well as ventilation images to the pre-RT planning CT image. It was presumed that the pre-
 RT plan was delivered until the 16-20 Gy scan acquisition, followed by delivery of the 16-20 Gy
 plan until the 30-34 Gy scan acquisition, and finally delivery of the 30-34 Gy plan until the end of
 treatment. To quantify the lung accumulated dose-function metrics with time-varying CT
 ventilation images before and during RT, a composite of dose-weighted ventilation was
 170 generated in this study. The composite ventilation (V_{comp}) in the voxel at location (x, y, z) of the
 pre-RT planning CT image is defined by

$$V_{comp}(x, y, z) = \sum_t \frac{D_t(x, y, z)}{D_{accum}(x, y, z)} V_t(x, y, z), \quad (1)$$

where t is the time point (*i.e.*, pre-RT, 16-20 Gy and 30-34 Gy), D_t is the dose of the pre-RT,
 16-20 Gy or 30-34 Gy plan, D_{accum} is the accumulated dose, and V_t is the ventilation obtained
 175 from the pre-RT, 16-20 Gy or 30-34 Gy scan.

Statistical analysis

Characteristics of tumor regression were evaluated to examine whether the manually-contoured
 GTV on the 16-20 Gy and 30-34 Gy planning CT images were significantly smaller than that of
 180 the pre-RT planning CT ($p < 0.05$) using the paired two-tailed t -test. The correlation between
 GTV changes and ventilation changes in the tumor-affected lung halves was also investigated
 using the Pearson correlation coefficient. Lung halves were segmented by dividing each of the
 right and left lungs into two parts at 4 cm below the carina, yielding four segments per patient.

Tumor-affected lung halves were defined as the segments that contained a tumor. Moreover, the accumulated dose metrics of the functional plans were compared with those of the anatomical plans for each scenario separately (functional adapted vs. anatomical adapted; and functional unadapted vs. anatomical unadapted) to investigate whether the difference was statistically significant ($p < 0.05$). The paired two-tailed t -test was used for the lung dose-function metrics that were found to meet the criteria for normality based on skewness and kurtosis [44,45]. The two-tailed Wilcoxon rank-sum test was used for all the other metrics, most of which did not meet the criteria for normality. The studied lung dose-function metrics include the functional mean lung dose (fMLD) (MLD weighted by regional ventilation) and fV_x (percentage of ventilation receiving $\geq x$ Gy).

Results

Tumor regression and regional ventilation changes

Figure 1 shows pre- and mid-RT (after 34 Gy) CT ventilation images of a representative case (patient 1) overlaid on the respective planning CT images. The GTV was 307 cm³ before RT, which was reduced by 48% to 158 cm³ after 34 Gy. Tumor shrinkage resulted in increases of regional ventilation as shown in Figure 1. The mean ventilation in the tumor-affected upper half of the left lung was 45% before RT, which was increased by 12% (relative increase) to 50%. For the 14 patients, the GTV was significantly reduced by 20% after 16-20 Gy ($p = 0.02$) and by 32% after 30-34 Gy ($p < 0.01$) on average. Figure 2 shows the relationship between GTV changes and ventilation changes in the tumor-affected lung halves measured with the two mid-RT CT scans for all patients except for patient 8, for which ventilation changes could not be calculated due to complete collapse of the ipsilateral lung. As GTV decreased, ventilation in the tumor-affected lung halves increased moderately but significantly ($r = -0.53$, $p < 0.01$).

Comparison of lung dose-function metrics

210 Figure 3 shows composite CT ventilation images (weighted by the functional adapted plan dose) overlaid on the planning CT images, accumulated dose distributions, and lung accumulated DFHs of the functional adapted and anatomical adapted plans for two representative patients. Patient 4 showed the largest reduction in the lung fV_{20} (5.6%) by functional plan adaptation compared to anatomical adaptation, while patient 6 showed the smallest reduction (1.4%).
215 Changes in the GTV and ventilation changes were comparable between the two patients, e.g., GTV reductions after 32 Gy were 44% for patient 4 and 49% for patient 6, and ventilation increases in the tumor-affected lung halves were 8.2% for patient 4 and 7.7% for patient 6.

Table 2 shows the average lung accumulated dose-function metrics of the functional adapted
220 and unadapted plans in comparison with the anatomical adapted and unadapted plans for 14 patients. The mean dose, fV_{10} , fV_{20} and fV_{30} were all found to be significantly lower in the functional adapted and unadapted plans than in the anatomical adapted and unadapted plans, respectively. On average, functional planning significantly reduced the accumulated fMLD by 5.0% ($p<0.01$) compared to anatomical planning in the adapted scenario, and by 3.6% ($p=0.03$)
225 in the unadapted scenario. Functional planning also resulted in significant reductions in the accumulated dose-volume metrics, e.g., MLD by 3.8% (13.3 ± 3.7 Gy vs. 13.8 ± 3.6 Gy, $p<0.01$) in the adapted scenario, and by 3.4% (14.0 ± 3.7 Gy vs. 14.5 ± 3.9 Gy, $p<0.01$) in the unadapted scenario.

230 *Comparison of dose-volume metrics of the CTV and other critical structures*

Table 3 shows the average accumulated dose-volume metrics of the CTV and other critical structures of the functional adapted and unadapted plans in comparison with the anatomical adapted and unadapted plans for 14 patients. The accumulated $D_{95\%}$ values of CTV, maximum dose to the spinal cord, mean dose to the esophagus, and V_{45} of the heart were all comparable
235 between the functional and anatomical plans in both scenarios. The accumulated $D_{95\%}$ values

of CTV were 1.5-2 Gy lower in the adapted plans than in the unadapted plans, because the CTV was determined by adding the same margin at each time point assuming that the microscopic disease shrank synchronously with the GTV. Note that the adapted and unadapted plans were not compared with each other for statistical significance in this study. The concern on the risk of underdosing microscopic tumor extension is discussed below in the Discussion section.

Discussion

This study demonstrated significant reductions in the functional lung dose with CT ventilation image-guided RT planning compared to anatomical image-guided planning in both scenarios with and without plan adaptation for patients showing tumor regression and changes in regional ventilation during a course of treatment. To our knowledge, this study is the first to quantify the dosimetric impact of changes in regional lung function during treatment as well as advantages of functional image-guided planning in two different scenarios with or without adaptation. The results suggest that functional image-guided planning, whether adapted or unadapted, may provide clinical benefit, *i.e.*, pulmonary toxicity reduction and quality of life improvement compared to anatomical image-guided planning. We only performed dosimetric evaluations in the present study, which is not sufficient but serves as an important first step in building the evidence for functional image-guided RT. Clinical trials will ultimately be necessary to determine its clinical significance. Several clinical trials are currently underway to investigate the feasibility or efficacy of lung functional image-guided RT without adaptation, *e.g.*, NCT02308709, 02528942, 02773238 and 02843568.

There are several limitations to the present study. First, treatment plans were created manually by an experienced dosimetrist, leading to a potential bias in favor of functional image-guided planning to reduce the lung dose more aggressively than anatomical image-guided planning. Functional image-guided planning resulted in significant reductions in not only the lung dose-

function metrics (e.g., functional mean lung dose) but also the dose-volume metrics (e.g., mean lung dose) as mentioned above. For future work, automated planning strategies [46-48] would allow for an unbiased, objective assessment. A recent study has successfully developed a knowledge-based planning model for lung functional image-guided RT [48]. Second, there are technical limitations to CT ventilation imaging, including 4D CT image artifacts that deteriorate the accuracy and precision of CT ventilation [31,49]. Future developments of strategies to improve 4D CT would improve CT ventilation imaging as well.

There are several challenges associated with adaptive RT strategies. A potential pitfall of adaptive RT is the risk of underdosing microscopic tumor extension. In this study, the CTV was determined by adding the same margin at each time point, assuming that the microscopic disease shrank synchronously with the GTV [21,22]. On the other hand, several other studies used DIR to propagate the CTV from the planning CT image before RT to the image during RT [22,50], considering that the microscopic disease might remain stationary [17]. Microscopic disease cannot be visualized with current imaging methods, leading to considerable uncertainties for individual patients. We maintained consistency in target volume coverage between the paired plans in each scenario, allowing for fair comparisons. Nevertheless, future developments of approaches to determine microscopic tumor extension are warranted to improve adaptive RT strategies. Additionally, the increased workload associated with replanning that typically requires a quick turnaround time poses a challenge in the clinical implementation of adaptive RT. Future developments of technologies to automate processes such as contouring, DIR and replanning may facilitate widespread implementation of adaptive RT. On the other hand, CT ventilation imaging has a greater availability compared to other modalities, which offers a particular strength in the implementation of functional image-guided adaptive RT.

Conclusions

This study demonstrated significant reductions in the accumulated dose to the functional lung
290 with CT ventilation functional image-guided treatment planning compared to standard
anatomical image-guided planning in two different scenarios with or without adaptation. The
findings of this study suggest the potential clinical benefit of functional image-guided plan
adaptation for locally advanced lung cancer, *i.e.*, pulmonary toxicity reduction and quality of life
improvement. Further studies, including clinical trials, are needed to determine its clinical
295 significance.

References

- [1] Mehta V. Radiation pneumonitis and pulmonary fibrosis in non-small-cell lung cancer: pulmonary function, prediction, and prevention. *Int J Radiat Oncol Biol Phys* 2005;63:5-24.
- 300 [2] Marks LB, Bentzen SM, Deasy JO, et al. Radiation dose-volume effects in the lung. *Int J Radiat Oncol Biol Phys* 2010;76:S70-76.
- [3] Palma DA, Senan S, Tsujino K, et al. Predicting radiation pneumonitis after chemoradiation therapy for lung cancer: an international individual patient data meta-analysis. *Int J Radiat Oncol Biol Phys* 2013;85:444-450.
- 305 [4] Jiang ZQ, Yang K, Komaki R, et al. Long-term clinical outcome of intensity-modulated radiotherapy for inoperable non-small cell lung cancer: the MD Anderson experience. *Int J Radiat Oncol Biol Phys* 2012;83:332-339.
- [5] Mazon R, Etienne-Mastroianni B, Perol D, et al. Predictive factors of late radiation fibrosis: a prospective study in non-small cell lung cancer. *Int J Radiat Oncol Biol Phys*
- 310 2010;77:38-43.
- [6] Marks LB, Yu X, Vujaskovic Z, et al. Radiation-induced lung injury. *Semin Radiat Oncol* 2003;13:333-345.
- [7] Marks LB, Spencer DP, Sherouse GW, et al. The role of three dimensional functional lung imaging in radiation treatment planning: the functional dose-volume histogram. *Int J Radiat*
- 315 *Oncol Biol Phys* 1995;33:65-75.
- [8] Seppenwoolde Y, Engelsman M, De Jaeger K, et al. Optimizing radiation treatment plans for lung cancer using lung perfusion information. *Radiother Oncol* 2002;63:165-177.
- [9] Ireland RH, Bragg CM, McJury M, et al. Feasibility of image registration and intensity-modulated radiotherapy planning with hyperpolarized helium-3 magnetic resonance
- 320 imaging for non-small-cell lung cancer. *Int J Radiat Oncol Biol Phys* 2007;68:273-281.
- [10] Bates EL, Bragg CM, Wild JM, et al. Functional image-based radiotherapy planning for non-small cell lung cancer: A simulation study. *Radiother Oncol* 2009;93:32-36.

- [11] Yamamoto T, Kabus S, von Berg J, et al. Impact of four-dimensional computed tomography pulmonary ventilation imaging-based functional avoidance for lung cancer radiotherapy. *Int J Radiat Oncol Biol Phys* 2011;79:279-288.
325
- [12] Faught AM, Miyasaka Y, Kadoya N, et al. Evaluating the Toxicity Reduction With Computed Tomographic Ventilation Functional Avoidance Radiation Therapy. *Int J Radiat Oncol Biol Phys* 2017;99:325-333.
- [13] Farr KP, Kallehauge JF, Moller DS, et al. Inclusion of functional information from perfusion SPECT improves predictive value of dose-volume parameters in lung toxicity outcome after radiotherapy for non-small cell lung cancer: A prospective study. *Radiother Oncol* 2015;117:9-16.
330
- [14] Faught AM, Yamamoto T, Castillo R, et al. Evaluating Which Dose-Function Metrics Are Most Critical for Functional-Guided Radiation Therapy. *Int J Radiat Oncol Biol Phys* 2017;99:202-209.
335
- [15] Theuws JC, Kwa SL, Wagenaar AC, et al. Dose-effect relations for early local pulmonary injury after irradiation for malignant lymphoma and breast cancer. *Radiother Oncol* 1998;48:33-43.
- [16] Zhang J, Ma J, Zhou S, et al. Radiation-induced reductions in regional lung perfusion: 0.1-12 year data from a prospective clinical study. *Int J Radiat Oncol Biol Phys* 2010;76:425-432.
340
- [17] Sonke JJ, Belderbos J. Adaptive radiotherapy for lung cancer. *Semin Radiat Oncol* 2010;20:94-106.
- [18] Vinogradskiy YY, Castillo R, Castillo E, et al. Use of weekly 4DCT-based ventilation maps to quantify changes in lung function for patients undergoing radiation therapy. *Med Phys* 2012;39:289-298.
345

- [19] Yuan ST, Frey KA, Gross MD, et al. Changes in global function and regional ventilation and perfusion on SPECT during the course of radiotherapy in patients with non-small-cell lung cancer. *Int J Radiat Oncol Biol Phys* 2012;82:e631-638.
- 350 [20] Meng X, Frey K, Matuszak M, et al. Changes in functional lung regions during the course of radiation therapy and their potential impact on lung dosimetry for non-small cell lung cancer. *Int J Radiat Oncol Biol Phys* 2014;89:145-151.
- [21] Guckenberger M, Wilbert J, Richter A, et al. Potential of adaptive radiotherapy to escalate the radiation dose in combined radiochemotherapy for locally advanced non-small cell lung cancer. *Int J Radiat Oncol Biol Phys* 2011;79:901-908.
- 355 [22] Guckenberger M, Richter A, Wilbert J, et al. Adaptive radiotherapy for locally advanced non-small-cell lung cancer does not underdose the microscopic disease and has the potential to increase tumor control. *Int J Radiat Oncol Biol Phys* 2011;81:e275-282.
- [23] Weiss E, Fatyga M, Wu Y, et al. Dose escalation for locally advanced lung cancer using adaptive radiation therapy with simultaneous integrated volume-adapted boost. *Int J Radiat Oncol Biol Phys* 2013;86:414-419.
- 360 [24] Simpson DR, Lawson JD, Nath SK, et al. Utilization of advanced imaging technologies for target delineation in radiation oncology. *J Am Coll Radiol* 2009;6:876-883.
- [25] Reinhardt JM, Ding K, Cao K, et al. Registration-based estimates of local lung tissue expansion compared to xenon CT measures of specific ventilation. *Med Image Anal* 2008;12:752-763.
- 365 [26] Fuld MK, Easley RB, Saba OI, et al. CT-measured regional specific volume change reflects regional ventilation in supine sheep. *J Appl Physiol* 2008;104:1177-1184.
- [27] Du K, Bayouth JE, Cao K, et al. Reproducibility of registration-based measures of lung tissue expansion. *Med Phys* 2012;39:1595-1608.
- 370 [28] Castillo R, Castillo E, Martinez J, et al. Ventilation from four-dimensional computed tomography: density versus Jacobian methods. *Phys Med Biol* 2010;55:4661-4685.

- [29] Castillo R, Castillo E, McCurdy M, et al. Spatial correspondence of 4D CT ventilation and SPECT pulmonary perfusion defects in patients with malignant airway stenosis. *Phys Med Biol* 2012;57:1855-1871.
- 375
- [30] Mathew L, Wheatley A, Castillo R, et al. Hyperpolarized (3)He magnetic resonance imaging: comparison with four-dimensional x-ray computed tomography imaging in lung cancer. *Acad Radiol* 2012;19:1546-1553.
- [31] Yamamoto T, Kabus S, von Berg J, et al. Reproducibility of four-dimensional computed tomography-based lung ventilation imaging. *Acad Radiol* 2012;19:1554-1565.
- 380
- [32] Kipritidis J, Siva S, Hofman MS, et al. Validating and improving CT ventilation imaging by correlating with ventilation 4D-PET/CT using (68)Ga-labeled nanoparticles. *Med Phys* 2014;41:011910.
- [33] Yamamoto T, Kabus S, Lorenz C, et al. Pulmonary Ventilation Imaging Based on 4-Dimensional Computed Tomography: Comparison With Pulmonary Function Tests and SPECT Ventilation Images. *Int J Radiat Oncol Biol Phys* 2014;90:414-422.
- 385
- [34] Vinogradskiy Y, Koo PJ, Castillo R, et al. Comparison of 4-dimensional computed tomography ventilation with nuclear medicine ventilation-perfusion imaging: a clinical validation study. *Int J Radiat Oncol Biol Phys* 2014;89:199-205.
- [35] Brennan D, Schubert L, Diot Q, et al. Clinical validation of 4-dimensional computed tomography ventilation with pulmonary function test data. *Int J Radiat Oncol Biol Phys* 2015;92:423-429.
- 390
- [36] Kida S, Bal M, Kabus S, et al. CT ventilation functional image-based IMRT treatment plans are comparable to SPECT ventilation functional image-based plans. *Radiother Oncol* 2016;118:521-527.
- 395
- [37] Kanai T, Kadoya N, Ito K, et al. Evaluation of four-dimensional computed tomography (4D-CT)-based pulmonary ventilation: The high correlation between 4D-CT ventilation and Kr-planar images was found. *Radiother Oncol* 2016.

- [38] Du K, Reinhardt JM, Christensen GE, et al. Respiratory effort correction strategies to
400 improve the reproducibility of lung expansion measurements. *Med Phys* 2013;40:123504.
- [39] *Detail omitted for blind review.*
- [40] *Detail omitted for blind review.*
- [41] Murphy K, van Ginneken B, Reinhardt JM, et al. Evaluation of registration methods on
thoracic CT: the EMPIRE10 challenge. *IEEE Trans Med Imaging* 2011;30:1901-1920.
- 405 [42] Guerrero T, Sanders K, Noyola-Martinez J, et al. Quantification of regional ventilation from
treatment planning CT. *Int J Radiat Oncol Biol Phys* 2005;62:630-634.
- [43] Simon BA. Non-invasive imaging of regional lung function using x-ray computed
tomography. *J Clin Monit Comput* 2000;16:433-442.
- [44] Trochim WMK Donnelly JP. The Research Methods Knowledge Base: Atomic Dog, 2006.
- 410 [45] Field A. Discovering Statistics Using SPSS: SAGE Publications, 2009.
- [46] Boylan C Rowbottom C. A bias-free, automated planning tool for technique comparison in
radiotherapy - application to nasopharyngeal carcinoma treatments. *J Appl Clin Med Phys*
2014;15:4530.
- [47] Sharfo AW, Voet PW, Breedveld S, et al. Comparison of VMAT and IMRT strategies for
415 cervical cancer patients using automated planning. *Radiother Oncol* 2015;114:395-401.
- [48] Faught AM, Olsen L, Schubert L, et al. Functional-guided radiotherapy using knowledge-
based planning. *Radiother Oncol* 2018.
- [49] Yamamoto T, Kabus S, Lorenz C, et al. 4D CT lung ventilation images are affected by the
4D CT sorting method. *Med Phys* 2013;40:101907.
- 420 [50] Hugo GD, Weiss E, Badawi A, et al. Localization accuracy of the clinical target volume
during image-guided radiotherapy of lung cancer. *Int J Radiat Oncol Biol Phys*
2011;81:560-567.

Figure legends

- 425 **Figure 1.** Pre- and mid-RT (after 34 Gy) CT ventilation images of a representative case (patient 1) overlaid on the respective planning CT images, which showed a 48% reduction in the tumor volume (red arrows) and a 12% increase in ventilation in the tumor-affected upper half of the left lung.
- 430 **Figure 2.** Gross tumor volume (GTV) changes vs. ventilation changes in the tumor-affected lung halves measured with two mid-RT CT scans (after 16-20 and 30-34 Gy) for all patients except for patient 8, for which ventilation changes could not be calculated due to complete collapse of the ipsilateral lung.
- 435 **Figure 3.** Composite CT ventilation images (weighted by the functional image-guided adapted plan dose), accumulated dose distributions, and lung accumulated dose-function histograms of the functional image-guided adapted and anatomical image-guided adapted plans for patient 4, showing the largest reduction in the lung functional V_{20} (5.6%) by functional image-guided adaptation. 10-30 Gy regions are pushed away from highly-functional lung regions (red arrows).
- 440 Patient 6 showed the smallest reduction (1.4%). Shaded red: clinical target volume (CTV).

Table 1. Patient characteristics

Parameter	Data
Age (y)	
Median	74
Range	57-84
Gender	
Male	6 (42.9)
Female	8 (57.1)
Stage	
IIIA	8 (57.1)
IIIB	6 (42.9)
Tumor location	
RUL	6 (42.9)
RLL	3 (21.4)
LUL	5 (35.7)
PTV (cm ³)	
Median	472
Range	255-750
Lung volume (cm ³)	
Median	2751
Range	2164-6287
Dose delivered prior to the 1st CT during RT (Gy)	
Median	18
Range	16-20
Dose delivered prior to the 2nd CT during RT (Gy)	
Median	32
Range	30-34

Abbreviations: RUL = right upper lobe; RLL; right lower lobe; LUL = left upper lobe; PTV = planning target volume, CT = computed tomography, RT = radiotherapy.

Data presented as the value of parameter or the number of patients with percentages in parentheses.

5

Table 2. Average lung accumulated dose-function metrics of the CT ventilation functional image-guided adapted and unadapted plans in comparison with the anatomical adapted and unadapted plans for 14 patients

Planning scheme	Mean (SD) (Gy)	fV ₁₀ (SD) (%)	fV ₂₀ (SD) (%)	fV ₃₀ (SD) (%)
Functional w/ adaptation	13.1 (3.9)	41.5 (14.3)	21.3 (8.6)	12.7 (5.7)
Anatomical w/ adaptation	13.8 (4.3)	44.3 (14.4)	23.8 (10.1)	13.8 (6.6)
<i>P</i> (vs. functional w/ adaptation)	<0.01	0.02	<0.01	<0.01
Functional w/o adaptation	13.9 (3.8)	43.6 (14.8)	23.1 (8.0)	13.9 (5.8)
Anatomical w/o adaptation	14.4 (4.2)	45.8 (15.0)	25.7 (10.2)	14.9 (6.3)
<i>P</i> (vs. functional w/o adaptation)	0.03	0.03	<0.01	<0.01

Abbreviation: SD = standard deviation; fV_x = percentage lung function receiving ≥x Gy.

Table 3. Average accumulated dose-volume metrics of the CTV and other critical structures of the CT ventilation functional image-guided adapted and unadapted plans in comparison with the anatomical adapted and unadapted plans for 14 patients

Planning scheme	CTV D _{95%} (SD) (Gy)	Spinal cord max (SD) (Gy)	Esophagus mean (SD) (Gy)	Heart V ₄₅ (SD) (%)
Functional w/ adaptation	58.9 (3.5)	36.7 (8.3)	24.6 (7.5)	3.2 (2.9)
Anatomical w/ adaptation	58.5 (3.6)	34.2 (8.9)	24.3 (7.3)	3.1 (2.8)
<i>P</i> (vs. functional w/ adaptation)	0.60	0.26	0.91	0.99
Functional w/o adaptation	60.6 (2.6)	38.3 (10.1)	26.3 (8.1)	3.4 (3.5)
Anatomical w/o adaptation	60.4 (2.6)	37.6 (9.7)	26.3 (8.0)	3.2 (3.0)
<i>P</i> (vs. functional w/o adaptation)	0.60	0.66	0.98	0.82

Abbreviation: CTV = clinical target volume; SD = standard deviation; D_{95%} = dose to 95% of the volume; V_x = percentage volume receiving ≥x Gy.

Summary: This paper reports on the first investigation to quantify the dosimetric advantages of computed tomography (CT) ventilation functional image-guided treatment planning for lung cancer in two different scenarios with or without plan adaptation. The results showed significant reductions in the accumulated dose to the functional lung with functional image-guided planning compared to anatomical image-guided planning in both scenarios for patients showing tumor regression and changes in regional ventilation during treatment.